Spectroscopic and Theoretical Studies of the Zn(II) Chelation with Hydroxyflavones

Christine Lapouge, Laetitia Dangleterre, and Jean-Paul Cornard*

LASIR, CNRS UMR 8516, Université des Sciences et Technologies de Lille, Bât C5-59655 Villeneuve d'Ascq Cedex, France

Received: July 11, 2006; In Final Form: September 14, 2006

The Zn(II) complexation of three naturally occurring organic compounds (3-hydroxyflavone, 5-hydroxyflavone, and 3′,4′-dihydroxyflavone) has been investigated by electronic spectroscopy combined with quantum chemical calculations. These three ligands, which differ in the nature of their chelating site, lead to the formation of a complex of 1:1 stoichiometry. The experimental results show that it is possible to class the three studied sites, according to their chelating power toward Zn(II), in the following way: α-hydroxy-carbonyl > β-hydroxy-carbonyl > catechol. Time-dependent density functional theory (TD-DFT) calculations were performed to obtain the excitation energies and oscillator strengths of the different complexes. Several effective core potentials (Los Alamos and Stuttgart/Dresden) were used for the description of the Zn ion. Calculations were also performed without any pseudopotential, and they give very satisfying results in the simulation of UV−vis spectra of the three complexes. Only the MWB28 ECP leads globally to a good quality description of the spectral features, roughly comparable to that obtained when the 6-31G(d,p) basis set is used to describe the Zn(II) orbitals. The analysis of the results shows that the nature of electronic transitions involved in the UV−vis spectra greatly differs according to the substitution pattern of the flavonoid.

1. Introduction

Flavonoids, 2-phenyl-benzo-α-pyrones, are polyphenolic molecules that occur ubiquitously in the plant kingdom; they are secondary metabolites of higher plants.[1,2] A multitude of substitution patterns in the two benzene rings (A and B) of the basic structure occur in nature. The individual compounds within each class are distinguished mainly by the number and orientation of hydroxyl, methoxyl, and other groups substituted in the two benzene rings. Flavonoids have attracted the attention of many researchers because of their numerous properties, notably biological properties.[3,4] These compounds are a group of phytochemicals with many antioxidant, antiviral, and antimutagenic agents.[5−8] Generally, it is assumed that the ability of flavonoids to chelate metals is very important for their antioxidant activity. Several authors have reported the chelation of Cu^{2+}, Fe^{2+}, and Fe^{3+} by various polyhydroxy-compounds.[9−17] For the hydroxyflavones, metal chelation occurs at the 3-hydroxy-4-keto, 5-hydroxy-4-keto binding sites or, if present, at vicinal dihydroxy sites of the B ring.[18−23] One of the difficulties that appears when dealing with a multisite ligand, a molecule possessing two or three chelating sites in competition, lies in the determination of the preferential site involved in the metal fixation. Our previous studies[24,25] have shown the efficiency of a methodology that combines electronic absorption spectroscopy and quantum chemical calculations for the Pb(II)−flavonoid system. In a continuation of this work, we focus on the Zn(II)−flavonoid system, and before taking up a study involving a multisite ligand, we were interested in the analysis of the complexation of monosite ligands to determine the best adapted computational conditions. A series of simple flavonoids has been selected to explore a systematic variation in the identity and spatial arrangement of metal-binding functional groups. The

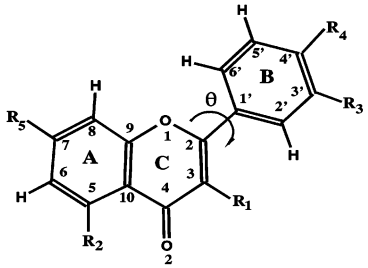

Compounds	R1	R2	R3	R4	R5
3-hydroxyflavone	OH	H	H	H	H
5-hydroxyflavone	H	OH	H	H	H
3',4'-dihydroxyflavone	H	H	OH	OH	H
quercetin	OH	OH	OH	OH	OH

Figure 1. Atomic numbering (IUPAC nomenclature) and substitution pattern of studied flavonoids.

3-hydroxyflavone (3HF), 5-hydroxyflavone (5HF), and 3′,4′-dihydroxyflavone (3′4′diHF) ligands, that, respectively, involve α-hydroxy-carbonyl, β-hydroxy-carbonyl, and catechol binding sites, have been investigated. The substitution pattern of the flavonoid ligands is shown in Figure 1. The goals of this study are (i) to compare the chelating power of these three sites toward Zn(II) ions using electronic absorption spectroscopy, (ii) to determine the structural changes of the ligands occurring with Zn(II) complexation, and (iii) to give an assignment of the spectral shifts observed in the UV−vis spectra of the ligands with the addition of metal. DFT and time-dependent DFT (TD-DFT) calculations were carried out to achieve the two last objectives. Another purpose of this study is also to determine the optimal conditions necessary for use in the quantum chemical calculations in order to obtain the best possible simulation of the electronic spectra of the flavonoid−Zn(II) complexes. Indeed, in further work, the quercetin molecule (Figure 1), that includes the three chelating sites in competition,

* Corresponding author. Phone: + 33-3.20.43.69.26. Fax: + 33-3.20.43.67.55. E-mail address: cornard@univ-lille1.fr.

10.1021/jp064362q CCC: $33.50
Published on Web 10/26/2006

will be studied so as to verify if the classification of the chelating power of the binding sites established from monosite ligands is preserved for a multisite ligand. For that, it is imperative to reproduce as well as possible the experimental spectra of complexes by TD-DFT calculations, to identify without ambiguity the preferential site implied in the fixation of Zn(II) by quercetin, only from the UV−vis spectrum of its complex.

2. Experimental Methods

The flavonoid compounds (3-hydroxyflavone, 5-hydroxyflavone, and 3′,4′-dihydroxyflavone) were purchased from Extrasynthese (France). Anhydrous zinc chloride was used without purification. Because of the very low solubility of these compounds in water, spectroscopic-grade methanol was used.

For each ligand, the molar ratio method has allowed us to determine the complex composition in solution from spectrophotometric measurements. For this method, solutions containing a constant concentration (4×10^{-5} M) of flavonoid in methanol and variable concentration of $ZnCl_2$ (from 4×10^{-7} to 1.2×10^{-4} M) were prepared. The complex stoichiometry has also been verified by the method of continuous variation (Job's method).

The UV−vis spectra were recorded on a Cary-l (Varian) spectrophotometer with cells of 1 cm path length, at 25 °C. A flow cell was used to allow successive additions of small amounts of Zn(II) chloride directly in the solution.

The formation constants of the complexes were estimated by using a multivariate data analysis program for modeling and fitting equilibrium titration 3D data sets obtained from the spectrophotometric measurements. The UV−vis spectra were refined using the SPECFIT software (version 3.0.32).[26] The set of spectra obtained at variable Zn(II) concentration was treated by the evolving factor analysis (EFA) method in order to determine the number of absorbing species in the system and the pure electronic spectrum of each species.[27,28] The Specfit software has also been used to estimate the stability constants (β's) and the standard deviation (σ). The stability constant estimation comes from the following reaction equation (where F is the flavonoid)

$$a\mathrm{Zn} + b\mathrm{F} \leftrightarrow \mathrm{Zn}_a\mathrm{F}_b$$

with the corresponding stability constant

$$\beta_{\mathrm{F}} = \frac{[\mathrm{Zn}_a\mathrm{F}_b]}{[\mathrm{Zn}]^a[\mathrm{F}]^b}$$

3. Computational Details

All the calculations reported in this paper have been performed using the GAUSSIAN (G03) program package.[29] Geometry optimizations of flavonoids and their complexes were carried out, without any symmetry constraints, using the 6-31G-(d,p) basis set (including polarization functions, to correctly take into account intramolecular H-bonding in the ligand). Three effective core potentials (ECPs) have been used to describe the Zn atom: the Los Alamos double-ξ LANL2DZ[30] which contains 18 core electrons and the MWB28 and MDF10 Stuttgart Dresden[31] with, respectively, 28 and 10 core electrons. The valence basis sets associated with these ECPs have the following contraction schemes: (3s2p5d)[2s2p2d], (4s2p)[3s2p], and (8s7p6d)[6s5p3d] for LANL2DZ, MWB28, and MDF10, respectively. The B3LYP exchange-correlation (XC) functional[32,33] was used for all the calculations. Vibrational frequency calculations have been performed to ensure that the optimized structures correspond to energy minima. The low-lying excited states were treated within the adiabatic approximation of time dependent density functional theory (DFT-RPA)[34] with the B3LYP hybrid functional. Vertical excitation energies were computed for the first 40 singlet excited states, to reproduce the UV−vis spectra of free and complexed ligands. Solvent effects on calculated UV−vis spectra were introduced by the SCRF method, via the polarized continuum model (PCM)[35] implemented in the Gaussian program.

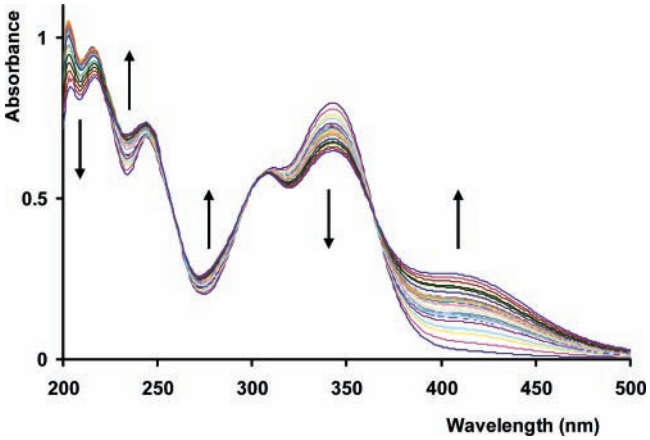

Figure 2. UV−vis spectra of 3′,4′-dihydroxyflavone in methanol in the absence and in the presence of $ZnCl_2$ for metal/ligand ratios varying from 0 to 5.

4. Results and Discussion

4.1. Zn(II) Complexation of Hydroxyflavones. The experimental spectra of the free ligands in methanol solution, as well as their theoretical spectra with assignments, have been already reported.[24] Here, we will focus only on the spectroscopic characterization of the complexes of the monosite flavonoids with Zn(II).

3′,4′-Dihydroxyflavone. Figure 2 illustrates the evolution of the UV−vis absorption spectra of the 3′4′diHF−Zn(II) system for different [Zn(II)]/[3′4′diHF] molar ratios, in methanol solution. The intensity of the band I, located at 343 nm, of free 3′4′diHF decreases with the amount of Zn(II) added, whereas a new band appears around 410 nm, characteristic of the complex. One can notice that the addition of $ZnCl_2$ modifies only very slightly the position in wavelength of the other absorption bands of the free ligand but varies their intensity. The obvious observation of an isosbestic point at 365 nm indicates the presence of an equilibrium between the free form and only one complex of 3′4′diHF. The molar ratio method has allowed us the determination of a 1:1 stoichiometry for this species. A numerical treatment of the electronic spectra set has been carried out to obtain the pure spectrum of the complex and its stability constant. A value of $\log \beta_{3'4'\mathrm{diHF}} = 5.19 \pm 0.09$ has been calculated for the $[\mathrm{Zn}(3'4'\mathrm{diHF})]^0$ complex in which the two hydroxyl functions on the B ring are deprotonated.

The spectrum of $[\mathrm{Zn}(3'4'\mathrm{diHF})]^0$ obtained from experimental data is presented in Figure 3 accompanied by the theoretical spectra calculated with the solvent effect (methanol) by using several basis sets. In a previous report,[36] we showed that the LANL2DZ ECP allowed a good description of the Zn^{2+} ion environment in the 3HF complex, and made it possible to obtain very good agreement between the theoretical electronic spectrum and the experimental spectrum of $[\mathrm{Zn}(3\mathrm{HF})]^+$. In the case of the 3′4′diHF complex, the experimental spectrum is very badly reproduced by the TD-DFT calculations when this pseudopo-

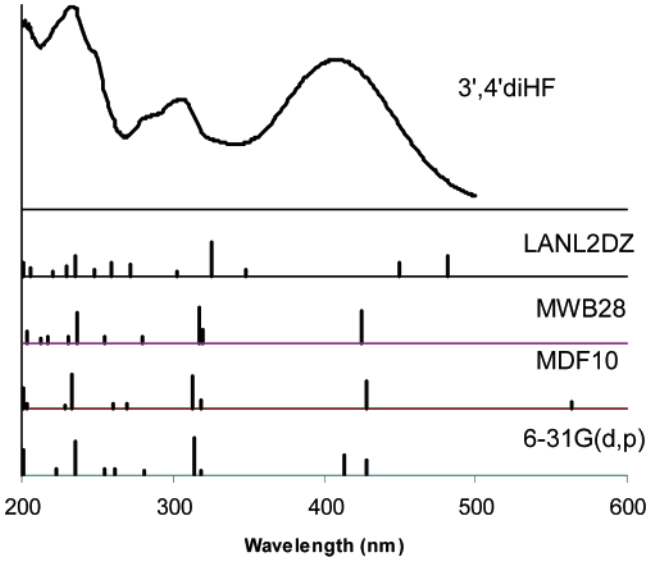

Figure 3. Experimental and theoretical spectra of $[Zn(3'4'diHF)]^0$ in methanol calculated with different metal/ligand basis sets: LANL2DZ/6-31G(d,p), MWB28/6-31G(d,p), MDF10/6-31G(d,p), and 6-31G(d,p)/6-31G(d,p).

tential is used. Notably, in the long wavelengths range, the transitions involving the HOMO and LUMO orbitals are calculated at 481 and 450 nm, values that must be compared to the broad absorption band observed at 410 nm. On the other hand, when the MWB28 Stuttgart/Dresden ECP is used, a better simulation of the complex electronic spectrum is observed. The long wavelengths absorption band is calculated only 15 nm too high with oscillator strength of 0.32. On the contrary, the MDF10 Stuttgart/Dresden ECP that includes 10 electrons in the core, leaving the outermost 18 electrons to be treated explicitly, gives rise to a calculated HOMO → LUMO transition at 563 nm. In all the cases, the MWB28 pseudopotential is better adapted to depict the electronic environment of the Zn atom coordinated to 3′4′diHF, and consequently, the electronic absorption spectrum of the complex than the LANL2DZ or MDF10 ECP. If no ECP is used for the Zn atom, the results show that the calculations carried out only with the 6-31G(d,p) basis set make it possible to obtain very good agreement between the theoretical and the experimental spectra of $[Zn(3'4'diHF)]^0$. All the features of the experimental spectrum are well reproduced with the 6-31G(d,p) (Figure 3), notably in wavelengths. It should be noted that, whatever the calculation method used, the transition corresponding to the band located to 309 nm is calculated with a value of the oscillator strength that is too high.

To observe the conformational changes of the ligand upon complexation, the main geometric parameters of the free ligand and complex calculated with the various basis sets are reported in Table 1. It is observed that the A and C rings (chromone moiety) are almost not affected by the complexation and the structural parameters of the corresponding chelate part are similar whatever the basis set. In the same way, the inter-ring bond does not undergo modification. For all the used basis sets, a very marked increase of the $C_{3'}C_{4'}$ bond length is calculated for $[Zn(3'4'diHF)]^0$, which induces modifications of the other bonds of the B ring. At the same time, a very important decrease of the CO bond lengths of the catechol group is observed with the metal fixation. One can notice that the calculations using the LANL2DZ and MDF10 basis sets give roughly the same results. It is the same when MWB28 and 6-31G(d,p) basis sets are employed. However, the geometry variations of the B ring

TABLE 1: Main Structural Parameters of Free and Complexed Forms of 3′,4′-Dihydroxyflavone[a]

		Zn(3′4′diHF)			
	3′4′diHF	lan12dz	MWB28	MDF10	6-31(d,p)
O_1C_2	1.366	1.366	1.367	1.366	1.367
C_2C_3	1.361	1.361	1.362	1.361	1.361
C_3C_4	1.455	1.456	1.455	1.457	1.457
C_4C_{10}	1.481	1.482	1.482	1.482	1.482
$C_{10}C_5$	1.403	1.404	1.403	1.404	1.403
C_5C_6	1.387	1.387	1.387	1.387	1.387
C_6C_7	1.405	1.405	1.405	1.405	1.405
C_7C_8	1.389	1.389	1.389	1.390	1.389
C_8C_9	1.398	1.399	1.400	1.399	1.398
C_9C_{10}	1.400	1.400	1.400	1.400	1.400
C_9C_1	1.372	1.372	1.371	1.372	1.372
$C_2C_{1'}$	1.472	1.471	1.471	1.471	1.470
$C_{1'}C_{2'}$	1.410	1.396	1.404	1.395	1.401
$C_{2'}C_{3'}$	1.384	1.405	1.395	1.405	1.395
$C_{3'}C_{4'}$	1.409	1.459	1.443	1.458	1.447
$C_{4'}C_{5'}$	1.392	1.414	1.403	1.413	1.403
$C_{5'}C_{6'}$	1.393	1.380	1.387	1.380	1.386
$C_{6'}C_{1'}$	1.404	1.425	1.414	1.425	1.414
C_4O_4	1.232	1.232	1.233	1.231	1.232
$C_{3'}O_{3'}$	1.375	1.317	1.349	1.319	1.346
$O_{3'}H_{3'}$	0.965				
$C_{4'}O_{4'}$	1.356	1.311	1.342	1.313	1.341
$O_{4'}H_{4'}$	0.970				
$O_{3'}Zn$		1.974	1.843	1.953	1.859
$O_{4'}Zn$		1.985	1.85	1.963	1.865
$O_{3'}$--$H_{4'}$	2.12				
$C_{3'}O_{3'}Zn$		104.3	100.9	103.7	100.1
$C_{4'}O_{4'}Zn$		104.1	100.9	103.6	100.0
$C_3C_2C_{1'}C_{2'}$	17.0	16.3	8.9	17.6	18.5
$C_{2'}C_{3'}O_{3'}Zn$		155.6	163.7	155.3	161.4

[a] Calculated with different basis sets for $[Zn(3'4'diHF)]^0$. The bond lengths are in ångstroms, and the bond angles and dihedral angles are in degrees.

are more pronounced for the LANL2DZ and MDF10 couple. Except for the calculation with MWB28, the inter-ring dihedral angle of the complex remains a value close to that calculated for 3′4′diHF. The $C_{3'}O_{3'}ZnO_{4'}C_{4'}$ ring is not calculated coplanar with the B ring, and the Zn atom leaves approximately 20° out of the plane. The $O_{4'}Zn$ bond is always found longer than the $O_{3'}Zn$ bond, however important discrepancies of the O−Zn lengths are observed according to the basis set used. In short, for $[Zn(3'4'diHF)]^0$, only the structures of the B ring and chelating site are affected by the metal binding. Nevertheless the conformational changes calculated for the Zn(II) chelation are more important than those found for the Pb(II) fixation on 3′4′diHF.[24]

5-Hydroxyflavone. The behavior of 5HF in the presence of zinc presents similarity with that of 3′4′diHF. With the addition of Zn(II), a new band appears at 402 nm which is characteristic of the complex formation, whereas the intensity of band I (337 nm) of the free ligand decreases (Figure 4). The other components of the electronic spectrum of the ligand present only subtle modifications, both in position and intensity, during the dosage. Once again, the presence of an isosbestic point at 358 nm lets us predict a simple equilibrium between the free ligand and a complexed form. The absorbance versus $[ZnCl_2]$/[5HF] molar ratio plots at different wavelengths (λ_{max} of free ligand and complex) made it possible to show the formation of a complex of 1:1 stoichiometry, whose formula is $[Zn(5HF)]^+$ with a deprotonated hydroxyl function. From chemometric analysis of the spectral data, the value of log β_{5HF} has been estimated to 5.33 ± 0.07. This value tends to indicate that the

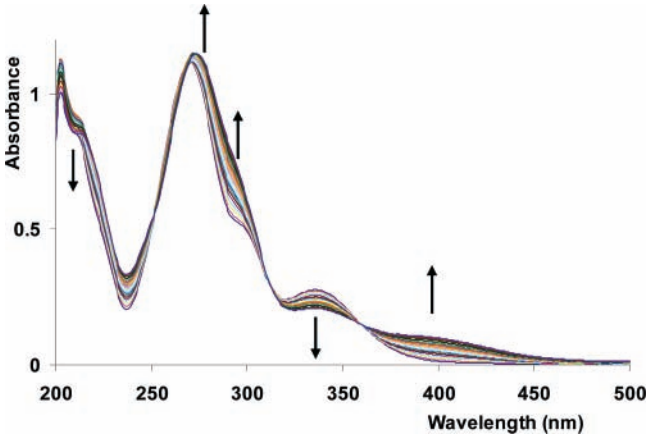

Figure 4. UV−vis spectra of 5-hydroxyflavone in methanol in the absence and in the presence of $ZnCl_2$ for metal/ligand ratios varying from 0 to 5.

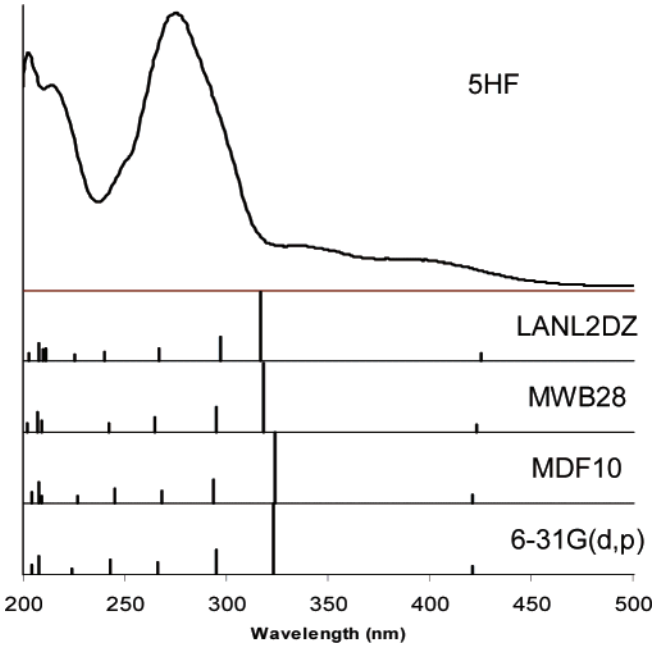

Figure 5. Experimental and theoretical spectra of $[Zn(5HF)]^+$ in methanol calculated with different metal/ligand basis sets: LANL2DZ/6-31G(d,p), MWB28/6-31G(d,p), MDF10/6-31G(d,p), and 6-31G(d,p)/6-31G(d,p).

β-hydroxy-carbonyl function presents a complexing capacity toward Zn(II) that is very slightly higher than that of the catechol function.

Just like for its homologous flavonoid, the theoretical spectrum of $[Zn(5HF)]^+$ has been calculated using different methods, with and without pseudopotential, and the results of these calculations are reported in Figure 5. In the long wavelengths range, the electronic spectrum of $[Zn(5HF)]^+$ obtained by spectral decomposition is characterized by two broad bands of very low intensity centered on 402 and 334 nm. Whatever the calculation method, these bands are not calculated in a completely satisfactory way. The first one is calculated with low oscillator strength (0.07 in average, value in good agreement with the experiment) but 20 nm too high with respect to the recorded wavelength. The second transition is calculated to be a little too low in wavelength (−10 nm for the better result), and especially with an oscillator strength value definitely too important (average: 0.64) compared to the absorption intensity. One can notice that the influence of the ECP on the electronic spectrum calculation is much less important for this complex than in the case of $[Zn(3'4'diHF)]^0$. Nevertheless, the use of the MDF10 pseudopotential gives results a little nearer to the experimental values than the other ECP. The spectral features in the low wavelengths range are, in a general way, relatively well described by all the calculations. When no pseudopotential is used for the description of the Zn atom, the results of the calculations at the 6-31G(d,p) level are quasi-identical to those obtained with the MDF10 ECP.

TABLE 2: Main Structural Parameters of Free and Complexed Forms of 5-Hydroxyflavone[a]

		$[Zn(5HF)]^+$			
	5HF	lan12dz	MWB28	MDF10	6-31G(d,p)
O_1C_2	1.361	1.341	1.341	1.340	1.341
C_2C_3	1.361	1.377	1.378	1.380	1.378
C_3C_4	1.477	1.410	1.408	1.405	1.405
C_4C_{10}	1.458	1.452	1.450	1.454	1.454
$C_{10}C_5$	1.422	1.449	1.448	1.449	1.451
C_5C_6	1.399	1.398	1.398	1.395	1.395
C_6C_7	1.395	1.392	1.393	1.393	1.392
C_7C_8	1.396	1.391	1.391	1.390	1.390
C_8C_9	1.391	1.387	1.387	1.388	1.387
C_9C_{10}	1.404	1.429	1.427	1.430	1.429
C_9C_1	1.374	1.369	1.369	1.368	1.369
$C_2C_{1'}$	1.476	1.460	1.460	1.458	1.458
$C_{1'}C_{2'}$	1.406	1.410	1.410	1.410	1.410
$C_{2'}C_{3'}$	1.391	1.390	1.389	1.389	1.389
$C_{3'}C_{4'}$	1.397	1.398	1.398	1.398	1.398
$C_{4'}C_{5'}$	1.395	1.397	1.397	1.398	1.397
$C_{5'}C_{6'}$	1.393	1.390	1.390	1.390	1.390
$C_{6'}C_{1'}$	1.406	1.409	1.410	1.410	1.410
C_4O_4	1.251	1.318	1.319	1.328	1.325
C_5O_5	1.338	1.350	1.349	1.361	1.358
O_5H_5	0.998				
O_4Zn		1.870	1.801	1.834	1.807
O_5Zn		1.838	1.772	1.805	1.781
O_4--H_5	1.684				
C_4O_4Zn		115.0	114.2	111.1	110.5
C_5O_5Zn		114.7	114.0	110.8	110.0
$C_3C_2C_{1'}C_{2'}$	19.9	10.6	11.1	10.2	10.0
$C_3C_4O_4Zn$		179.8	179.7	179.9	179/8

[a] Calculated with different basis sets for $[Zn(5HF)]^+$. The bond lengths are in ångstroms, and the bond angles and dihedral angles are in degrees.

The structural modifications of 5HF engendered by the metal fixation are presented in Table 2. As expected, the B ring is not affected by the complex formation. The coordination of Zn(II) at the level of the C═O, which sees a strong increase of its bond length, results in an electronic redistribution mostly on the C ring. For instance, the C_3O_4 bond length decreases in an important way, while the $C_{10}C_5$ increases. The two C—O bonds in the chelate present very different lengths; the C_4O_4 always remains shorter than the C_5O_5 bond. Contrary to what was observed in the formation of $[Zn(3'4'diHF)]^0$, the chelate ring is planar, and the zinc atom is located in the chromone part plane. The inter-ring bond length slightly decreases, and the B ring is less twisted in the complex than in 5HF. The basis set influence on the structural features of $[Zn(5HF)]^+$ is much less important than that observed in the case of $[Zn(3'4'diHF)]^0$, except for the O—Zn bond lengths that show disparities which can reach 0.07 Å according to the basis set used. However, in all the cases, it is observed that O_4Zn is calculated longer than O_5Zn.

3-Hydroxyflavone. The study of the Zn(II) chelation by the α-hydroxy-carbonyl site will not be detailed insofar as the $[Zn(3HF)]^+$ complex was the object of a already published letter.[36] We showed that the introduction of LANL2DZ pseudopotential into calculations made it possible to very well reproduce the experimental absorption spectrum of the Zn-3HF system. The

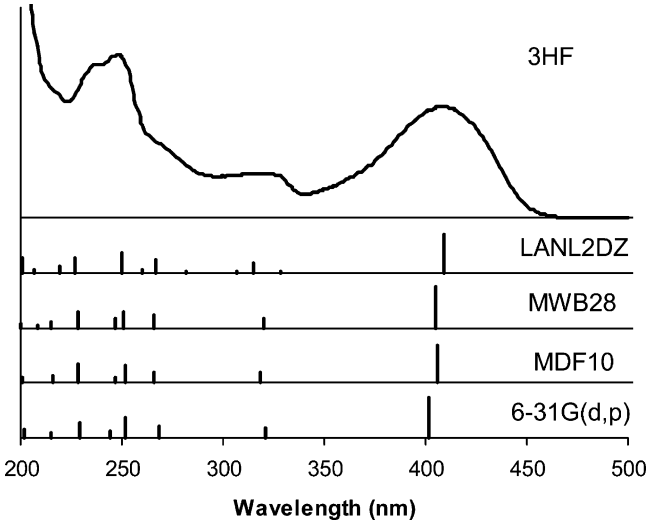

Figure 6. Experimental and theoretical spectra of $[Zn(3HF)]^+$ in methanol calculated with different metal/ligand basis sets: LANL2DZ/6-31G(d,p), MWB28/6-31G(d,p), MDF10/6-31G(d,p), and 6-31G(d,p)/6-31G(d,p).

TABLE 3: Main Structural Parameters of Free and Complexed Forms of 3-hydroxyflavone (calculated with different basis sets for $[Zn(3HF)]^+$[a]

		$[Zn(3HF)]^+$			
	3HF	lan12dz	MWB28	MDF10	6-31G(d,p)
C_3O_3	1.352	1.341	1.354	1.338	1.358
C_4O_4	1.243	1.308	1.319	1.306	1.321
O_3Zn		1.902	1.816	1.897	1.831
O_4Zn		1.935	1.843	1.928	1.858
$C_3C_2C_{1'}C_{2'}$	0	15.7	1.7	16.7	13.6
$C_2C_3O_3Zn$		165.6	179.7	161.6	176.5

[a] See also ref 36. The bond lengths are in ångstroms, and the bond angles and dihedral angles are in degrees.

same calculations were carried out again with the Stuttgart Dresden ECPs and without pseudopotential. The calculated transitions using different basis sets for the Zn atom (Figure 6) show very little difference, in wavelength as for the oscillator strength. That tends to say that the basis set effect is negligible in the electronic description of this system, whereas much more marked differences were observed for the preceding systems, notably the $[Zn(3'4'diHF)]^0$ complex.

Insofar as the comparison of the structures of the free and complexed ligands were already published, we only report, in Table 3, the geometrical parameters which show significant differences according to the basis set used. The only structural modifications are observed on the level of the fixation site; the parameters of the ligand (and notably the bond lengths) are very slightly affected by the choice of the basis set. As in the case of $[Zn(3'4'diHF)]^0$, one can identify two distinct couples (LANL2DZ, MDF10 and MWB28, 6-31G(d,p)) which give rather similar results. However, it should be noted that a quasiplanar structure of the complex is calculated with the MWB28 ECP, whereas the other basis sets lead to a twisted structure. The fact that the theoretical electronic spectra, calculated with the various basis sets, show very little difference tends to show that the inter-ring dihedral angle value has a very weak influence on the electronic transitions.

4.2. Comparison of the Flavonoid Complexes. The three studied monosite flavonoids chelate the Zn ion to form a complex of 1:1 stoichiometry. A straightforward comparison of the conditional stability constants of these complexes allows classifying the ligands according to their complexation capacity. The α-hydroxy-carbonyl function is unambiguously the site that presents the most important chelating ability toward Zn(II) (log $\beta_{3HF} = 6.60 \pm 0.10$).[36] The β-hydroxy-carbonyl and catechol functions have very close complexation capacities, with a slight advantage in favor of the first site. Thus, it is possible to class the three sites in the following way: α-hydroxy-carbonyl > β-hydroxy-carbonyl > catechol.

The Gibbs free energies of the complexation reactions of 3HF and 5HF ligands (noted AH) have been calculated at the B3LYP/6-31G(d,p) level of theory, taking into account the solvent effects and according to the following reaction:

$$Zn^{2+} + AH + MeOH \Leftrightarrow AZn^+ + MeOH_2^+$$

The calculated Gibbs energy are −10.2 and −4.7 kcal.mol^{-1} for 3HF and 5HF, respectively. In methanol, the complexation reaction of 3HF is more exergonic than of 5HF, in good agreement with the relative stability observed for the corresponding complexes. However, these values cannot be directly connected to the stability constants insofar as these constants are conditional. On the other hand, the Gibbs free energy of the complexation reaction of 3′4′diHF cannot be compared to the previous ones as the complexation of this ligand occurs with a double deprotonation of the chelating site.

The chelating power order of the sites established for Zn^{2+} is the same as that observed for the complexation of Al(III),[37] except that a complex $[Al(3HF)_2]^+$ was obtained for the 3HF ligand. In contrast, among the three sites, the catechol function presents the greatest chelating power toward Pb(II) and leads to the formation of $[Pb(3'4'diHF)]^0$.[38] As expected, the chelating ability order of the three studied sites depends on the metal ion, but this order can also be largely influenced by the physicochemical conditions, such as pH for instance. Consequently, this study, having been undertaken in a neutral medium, can in no case be extrapolated in other conditions.

From a structural point of view, generally, the geometry of the ring carrying the chelating group is the most affected by the complexation. The structural modifications follow the same trends but are more or less marked according to the basis set used. Only the environment of the zinc atom (Zn−O bond lengths, dihedral angle of the chelate ring) presents important changes with the basis set. If, for some flavonoid compounds, the introduction of a pseudopotential makes it possible to obtain good results in the simulation of the electronic spectrum of the complexes with the Zn(II) ion, it should be noted that the 6-31G(d,p) basis set allows the most satisfactory description of the whole of the experimental data presented in this work. This result tends to show that to determine the preferential chelating site of a multisite flavonoid (such as quercetin) which presents the three sites in competition toward Zn(II), it will be preferable to avoid the use of an ECP for the metal description or possibly the MWB28 pseudopotential that gives results relatively close to those found with the 6-31G(d,p) basis set for all the studied compounds. So, in the continuation of this paper, we will only discuss the results obtained without ECP.

If we only focus on the absorption band located in the long wavelengths, which is characteristic of the complex insofar as it appears with the addition of metal, one observes that this one is described by two electronic transitions in the case of $[Zn(3'4'diHF)]^0$ and only one for the two other complexes (Table 4). For $[Zn(5HF)]^+$ and $[Zn(3HF)]^+$, the HOMO → LUMO is the only preponderant transition, whereas the HOMO → LUMO + 1 transition also presents a very important contribution to the assignment of the long wavelengths absorption band of $[Zn(3'4'diHF)]^0$. It is interesting to note that the oscillator strengths

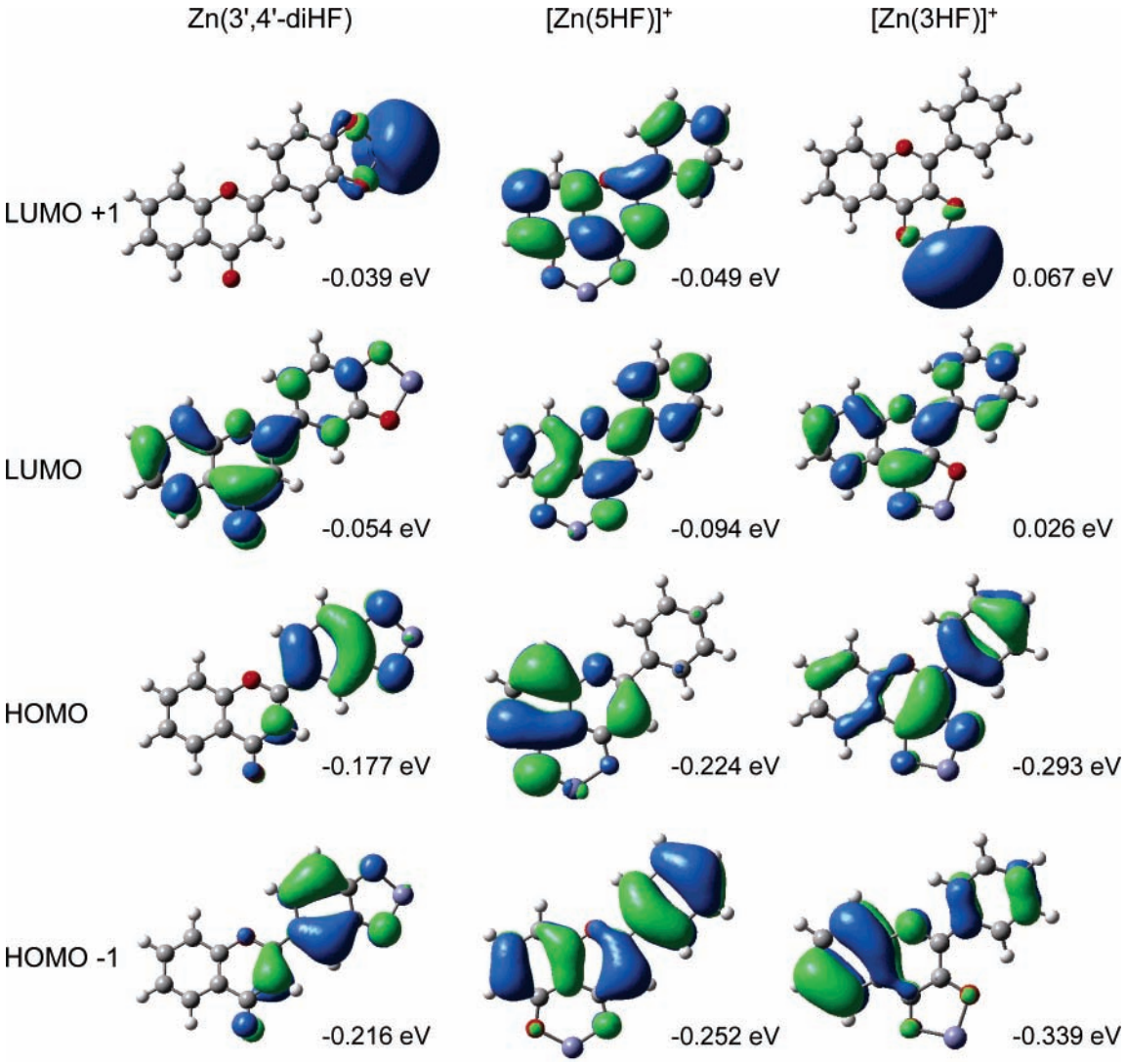

Figure 7. Molecular frontier orbitals (with their energy) involved in the electronic transitions of the $[Zn(3'4'diHF)]^0$, $[Zn(5HF)]^+$, and $[Zn(3HF)]^+$.

TABLE 4: Experimental and Calculated Wavelengths in Gas Phase and with Solvent Effects of the Absorption Band in the Long Wavelength Range of the Three Studied Complexes and Molecular Orbitals Involved in the Electronic Transitions

	expt λ (nm)	gas phase λ_{cal} (nm)	with solvent effects		
			λ_{cal} (nm)	f[a]	MO contribution
$[Zn(3'4'\text{-diHF})^0$	410	346	428	0.15	H → L + 1 (71%)
					H → L (25%)
			414	0.19	H → L (64%)
					H → L + 1 (26%)
$[Zn(5HF)]^+$	402	342	420	0.08	H → L (92%)
$[Zn(3HF)]^+$	408	390	402	0.48	H → L (80%)

[a] *f* is the oscillator strength.

calculated for the three complexes well describe the relative intensity of these absorption bands; indeed, the most important intensity is observed for the complex of 3HF,[36] followed by the 3′4′diHF, and finally the absorbance of the $[Zn(5HF)]^+$ band is very weak. The complex spectra have also been calculated in the gas phase, and the values of the absorption wavelengths are reported in Table 4. These calculated values are very far from the experimental ones, and for instance, the HOMO → LUMO transition is calculated at 1617 nm with a very low oscillator strength, and the first non-negligible transition appears at 390 nm for the 3HF complex. As expected, a good simulation

TABLE 5: Mulliken Analysis (B3LYP/6-31G(d,p)) of the Contribution of the Different Parts of the Molecule (Chromone, B ring, and Zn atom) to the Frontier Molecular Orbitals Involved in the Transition Observed in the Long Wavelength Range of $[Zn(3'4'diHF)]^0$, $[Zn(5HF)]^+$, and $[Zn(3HF)]^+$

	$[Zn(3'4'di\ HF)]^0$			$[Zn(5HF)]^+$		$[Zn(3HF)]^+$	
	HOMO	LUMO	LUMO + 1	HOMO	LUMO	HOMO	LUMO
chromone	9.81	80.73	0.86	97.33	79.09	79.82	81.11
B ring	87.27	18.61	22.84	1.26	20.81	18.65	18.56
Zn atom	2.92	0.66	76.3	1.41	0.1	1.53	0.33

of the electronic spectra necessitates to take into account the solvent effects.

The nature of the electronic transitions which are at the origin of the long wavelengths band of the complexes completely differs for the three studied ligands (Figure 7). For $[Zn(3'4'diHF)]^0$, the transitions are characterized by a charge transfer from the B ring to the chromone part (HOMO → LUMO) or from the B ring to the Zn atom (HOMO → LUMO + 1). Indeed, in the HOMO, 87% of the electronic density is localized on the B-ring, whereas the most important electronic density is found on the chromone part (81%) and on the Zn atom (76%) in the LUMO and LUMO + 1, respectively (Table 5). For $[Zn(5HF)]^+$, the HOMO → LUMO transition consists of a charge transfer from the chromone part to the B ring, where the contribution to the B ring increases from 1% (HOMO) to 21%

(LUMO). Both HOMO and LUMO are delocalized on the whole of the ligand for $[Zn(3HF)]^+$ as shown by the population of these molecular orbitals which are very similar. In these two last cases, the electronic transition has a $\pi\pi^*$ character. As the LUMO + 1 of $[Zn(3'4'diHF)]^0$, the LUMO + 1 of $[Zn(3HF)]^+$ is totally localized on the Zn atom; however, this MO does never participate in the low-lying optical excitation calculated with a non-negligible transition probability for this complex. It is worth noting that the Mulliken analysis of the frontier molecular orbitals has been carried out without ECP; the same calculations performed with a pseudopotential give similar results except for the 3′4′diHF complex with LANL2DZ ECP. Indeed, the use of this pseudopotential leads to significant modifications of the electronic distribution especially in the LUMO + 1. This fact induces a change in the MO's energy and consequently could explain the lesser agreement between the experimental spectrum of $[Zn(3'4'diHF)]^0$ and the theoretical one calculated with LANL2DZ pseudopotential.

4. Conclusion

The results presented in this work provide further information regarding the complexation of Zn(II) ions with some hydroxyflavones. All of the ligands lead to the formation of complex of 1:1 stoichiometry, and the comparison of the formation constants has allowed a classification of the three binding sites with respect to their chelating power. The α-hydroxy-carbonyl site presents the greatest affinity for Zn(II) ion. The simulation of the electronic spectra of the complexes shows that the three used pseudopotentials do not give results with the same accuracy for the three compounds. However, the MWB28 ECP leads globally to a satisfying description of spectral features, roughly comparable to those obtained with all electron calculations. In such conditions, the study of the Zn(II) complexation by quercetin (multibinding site ligand) will be performed without any ECP to ensure the best computational conditions. The comparison of the UV−vis spectrum of the Zn(II)−quercetin system with the three theoretical spectra calculated with a chelation of Zn atom on each site would exhibit the preferential complexing function. This approach was already used successfully on the Pb(II)−quercetin system[25] and has shown that the catechol group was the most powerful chelating site toward Pb(II) in this multisite ligand as it was predicted by the studies of the monosite ligands. It can noted that Le Nest et al.[39,40] have already reported studies of the Zn(II) chelation by quercetin in different hydro-organic solvents buffered at pH 7, and have found the formation of binuclear complexes; they suggested that the α-hydroxy-carbonyl site is preferentially involved.

Acknowledgment. "Institut du Développement et des Ressources en Informatique Scientique" (IDRIS-Orsay, France) is thankfully acknowledged for the CPU time allocation. The authors also thank the Lille University Computational Center (C.R.I.).

References and Notes

(1) Haslam, E. *Plant Polyphenols. Vegetable Tannins Revisited*; Cambridge University Press: Cambridge, U. K., 1989.
(2) Larson, R. A. *Phytochemistry* **1988**, *27*, 969.
(3) Leighton, T.; Ginther, C.; Fluss, L.; Harter, W.; Cansado, J.; Notario, V. Phenolic Compounds in Foods and their Effects on Health II. In *ACS Symposium Series 507*; Huang, T., Ho, C. T., Lee, C. Y., Eds.; American Chemical Society: Washington, DC, 1992.
(4) Moreira, A. J.; Fraga, C.; Alonso, M.; Collado, P. S.; Zetller, C.; Marroni, C.; Maronni, N.; Gonzalez-Gallego, J. *Biochem. Pharmacol.* **2004**, *68*, 1939.
(5) Bors, W.; Heller, W.; Michel, C.; Saran, M. *Methods Enzymol.* **1990**, 343.
(6) Cos, P.; Yi, L.; Calomme, M.; Hu, J. P.; Cimanga, K.; Poel, B.; Pieters, L.; Vlietinck, A. J.; Berghe, V. *J. Nat. Prod.* **1998**, *61*, 71.
(7) Ko, F.; Chu, C.; Lin, C.; Chang, C.; Teng, C. *Biochim. Biophys. Acta* **1988**, *1389*, 81.
(8) Rice-Evans, C.; Miller, N.; Paganga, G. *Trends Plant Sci.* **1997**, *2*, 152.
(9) Barhacs, L.; Kaizer, J.; Pap, J.; Speier, G. *Inorg. Chim. Acta* **2001**, *320*, 83.
(10) Moridani, M. Y.; Pourahmad, J.; Bui, H.; Siraki, A.; O'Brien, P. J. *Free Radical Biol. Med.* **2003**, *34*, 243.
(11) Rice-Evans, C. A.; Miller, N. J.; Paganga, G. *Free Radical Biol. Med.* **1996**, *20*, 933.
(12) Jungbluth, G.; Rühling, I.; Ternes, W. *J. Chem. Soc., Perkin Trans. 2* **2000**, 1946.
(13) Engelmann, M. D.; Hutcheson, R.; Cheng, F. *J. Agric. Food Chem.* **2005**, *53*, 2953.
(14) Leopoldini, M.; Russo, N.; Chiodo, S.; Toscano, M. *J. Agric. Food Chem.* **2006**, *54*, 6343.
(15) Zhou, J.; Wang, L.; Wang, J.; Tang, N. *Transition Met. Chem.* **2001**, *26*, 57.
(16) de Souza, R. F. V.; Sussuchi, E. M.; De Giovani, W. F. *Synth. React. Inorg. Met.-Org. Chem.* **2003**, *33*, 1125.
(17) Khokhar, S.; Owusu Apenten, R. K. *Food Chem.* **2003**, *81*, 133.
(18) Castro, G. T.; Blanco, S. E. *Spectrochim. Acta, Part A* **2004**, *60*, 2235.
(19) Balogh-Hergovich, E.; Kaizer, J.; Speier, G. *J. Mol. Catal. A: Chem.* **2000**, *159*, 215.
(20) De Souza, R. F. V.; De Giovani, W. F. *Spectrochim. Acta, Part A* **2005**, *61*, 1985.
(21) Viswanathan, P.; Sriram, V.; Yogeeswaran, G. *J. Agric. Food Chem.* **2000**, *48*, 2802.
(22) Hollman, P. C. H.; van Trijp, J. M. P.; Buysman, M. N. C. P. *Anal. Chem.* **1996**, *68*, 3511.
(23) Roshal, A. D.; Grigorovich, A. V.; Doroshenko, A. O.; Pivovarenko, V. G.; Demchenko, A. P. *J. Phys. Chem. A* **1998**, *102*, 5907.
(24) Lapouge, C.; Cornard, J. P. *J. Phys. Chem. A* **2005**, *109*, 6752.
(25) Cornard, J. P.; Dangleterre, L.; Lapouge, C. *J. Phys. Chem. A* **2005**, *109*, 10044.
(26) Specfit Global Analysis System, S. S. A., Marlborough, MA.
(27) Gampp, H.; Maeder, M.; Meyer, C. J.; Zuberbühler, A. *Talanta* **1985**, *32*, 1133.
(28) Gampp, H.; Maeder, M.; Meyer, C. J.; Zuberbühler, A. *Talanta* **1986**, *33*, 943.
(29) Gaussian 03, R. B.; Frisch, M. J.; Trucks, G. W.; Schlegel, H. B.; Scuseria, G. E.; Robb, M. A.; Cheeseman, J. R.; Montgomery, J., J. A.; Vreven, T.; Kudin, K. N.; Burant, J. C.; Millam, J. M.; Iyengar, S. S.; Tomasi, J.; Barone, V.; Mennucci, B.; Cossi, M.; Scalmani, G.; Rega, N.; Petersson, G. A.; Nakatsuji, H.; Hada, M.; Ehara, M.; Toyota, K.; Fukuda, R.; Hasegawa, J.; Ishida, M.; Nakajima, T.; Honda, Y.; Kitao, O.; Nakai, H.; Klene, M.; Li, X.; Knox, J. E.; Hratchian, H. P.; Cross, J. B.; Bakken, V.; Adamo, C.; Jaramillo, J.; Gomperts, R.; Stratmann, R. E.; Yazyev, O.; Austin, A. J.; Cammi, R.; Pomelli, C.; Ochterski, J. W.; Ayala, P. Y.; Morokuma, K.; Voth, G. A.; Salvador, P.; Dannenberg, J. J.; Zakrzewski, V. G.; Dapprich, S.; Daniels, A. D.; Strain, M. C.; Farkas, O.; Malick, D. K.; Rabuck, A. D.; Raghavachari, K.; Foresman, J. B.; Ortiz, J. V.; Cui, Q.; Baboul, A. G.; Clifford, S.; Cioslowski, J.; Stefanov, B. B.; Liu, G.; Liashenko, A.; Piskorz, P.; Komaromi, I.; Martin, R. L.; Fox, D. J.; Keith, T.; Al-Laham, M. A.; Peng, C. Y.; Nanayakkara, A.; Challacombe, M.; Gill, P. M. W.; Johnson, B.; Chen, W.; Wong, M. W.; Gonzalez, C.; Pople, J. A.; Gaussian 03, Revision B.04 ed.; Gaussian InC., Pittsburgh, PA, 2003.
(30) Hay, P. J.; Wadt, W. R. *J. Chem. Phys.* **1985**, *82*, 270.
(31) Dolg, M.; Wedig, U.; Stoll, H.; Preuss, H. *J. Chem. Phys.* **1987**, *86*, 866.
(32) Becke, A. D. *J. Chem. Phys.* **1993**, *98*, 5648.
(33) Lee, C.; Yang, W.; Parr, R. G. *Phys. Rev. B* **1988**, *37*, 785.
(34) Bauernschmitt, R.; Ahlrichs, R. *Chem. Phys.* **1996**, *256*, 454.
(35) Cossi, M.; Scalmani, G.; Rega, N.; Barone, V. *J. Chem. Phys.* **2002**, *117*, 43.
(36) Cornard, J. P.; Dangleterre, L.; Lapouge, C. *Chem. Phys. Lett.* **2006**, *419*, 304.
(37) Cornard, J. P.; Merlin, J. C. *J. Mol. Struct.* **2003**, *651*−*653*, 381.
(38) Dangleterre, L.; Cornard, J.-P. *Polyhedron* **2005**, *24*, 1593.
(39) Le Nest, G.; Caille, O.; Woudstra, M.; Roche, S.; Burlat, B.; Belle, V.; Guigliarelli, B.; Lexa, D. *Inorg. Chim. Acta* **2004**, *357*, 2027.
(40) Le Nest, G.; Caille, O.; Woudstra, M.; Roche, S.; Guerlesquin, F.; Lexa, D. *Inorg. Chim. Acta* **2004**, *357*, 775.